Journal Pre-proof

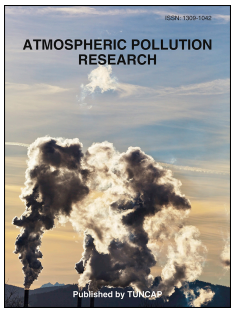

Occurrence, sources and seasonal variation of $PM_{2.5}$ carbonaceous aerosols in a water level fluctuation zone in the Three Gorges Reservoir, China

Xi Wang, Fengwen Wang, Ting Feng, Siyuan Zhang, Zhigang Guo, Peili Lu, Li Liu, Fumo Yang, Jiaxin Liu, Neil L. Rose

PII: S1309-1042(20)30099-4

DOI: https://doi.org/10.1016/j.apr.2020.04.014

Reference: APR 791

To appear in: *Atmospheric Pollution Research*

Received Date: 27 November 2019

Revised Date: 20 April 2020

Accepted Date: 21 April 2020

Please cite this article as: Wang, X., Wang, F., Feng, T., Zhang, S., Guo, Z., Lu, P., Liu, L., Yang, F., Liu, J., Rose, N.L., Occurrence, sources and seasonal variation of $PM_{2.5}$ carbonaceous aerosols in a water level fluctuation zone in the Three Gorges Reservoir, China, *Atmospheric Pollution Research* (2020), doi: https://doi.org/10.1016/j.apr.2020.04.014.

Xi Wang: Writing-Original draft preparation.
Fengwen Wang: Supervision.
Ting Feng: Sample collection.
Siyuan Zhang: Sample treatment in lab.
Peili Lu: Table 1 and Table 2 data collection.
Fumo Yang: Figures 1-5 integration.
Jiaxin Liu and Zhigang Guo: Data analyzing.
Neil L. Rose: Grammar check and language polishing.
Li Liu: Reviewing and editing.

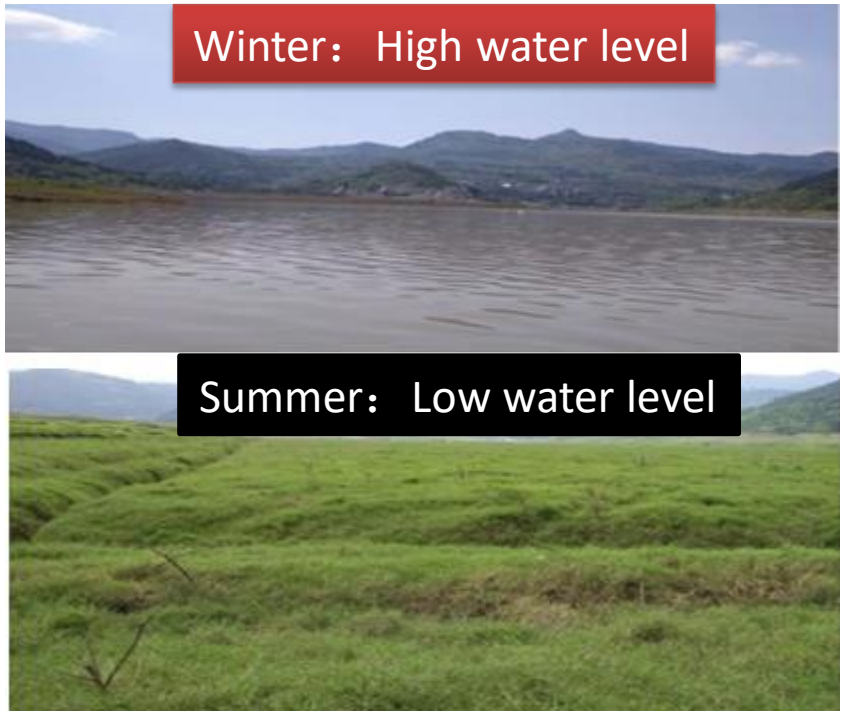

water-level-fluctuation zone (WLFZ) in TGRR

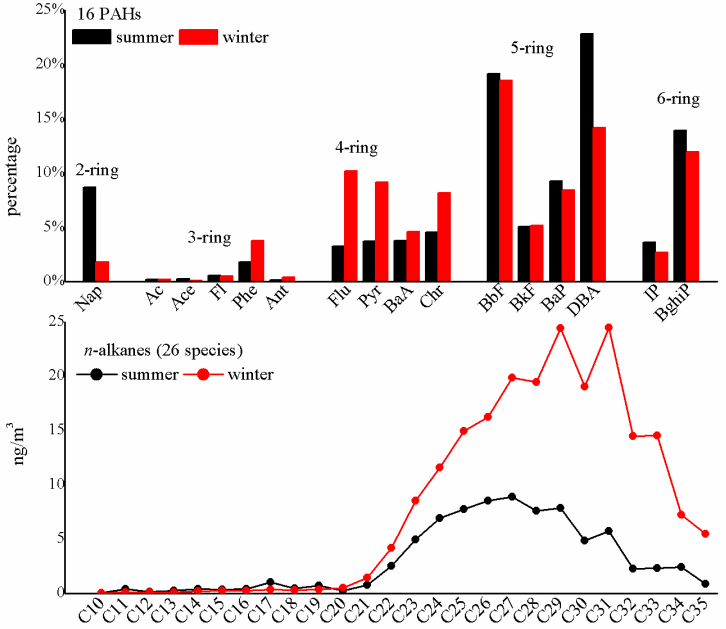

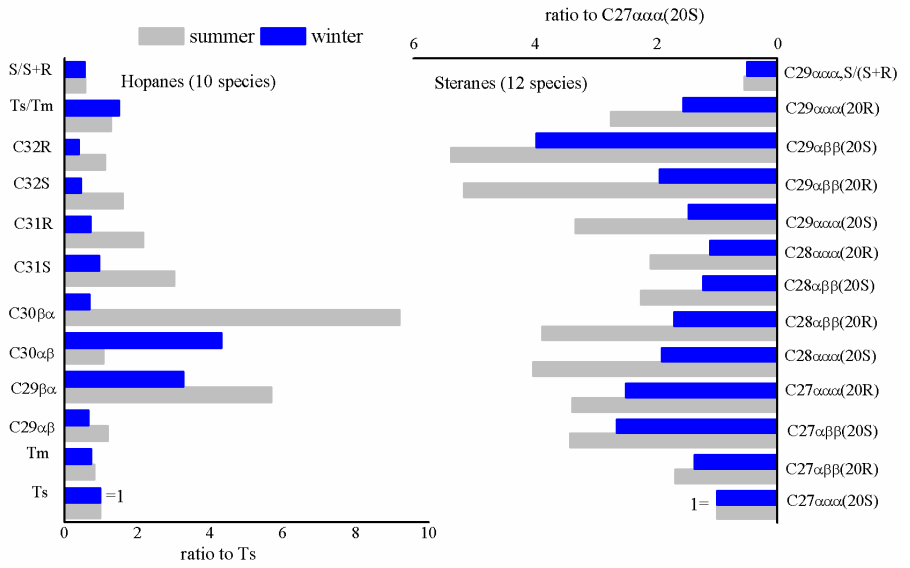

Occurrence, sources and seasonal variation of $PM_{2.5}$ carbonaceous aerosols in a water level fluctuation zone in the Three Gorges Reservoir, China

Xi Wang[ab], Fengwen Wang[ac*], Ting Feng[c], Siyuan Zhang[c], Zhigang Guo[d], Peili Lu[ac], Li Liu[ab], Fumo Yang[e], Jiaxin Liu[f], Neil L. Rose[g]

[a]State Key Laboratory of Coal Mine Disaster Dynamics and Control, Chongqing University, Chongqing 400030, China

[b]College of Resources and Safety Engineering, Chongqing University, Chongqing 400030, China

[c]Department of Environmental Science, Chongqing University, Chongqing 400030, China

[d]Department of Environmental Science and Engineering, Fudan University, Shanghai 200433, China

[e]Department of Environmental Science and Engineering, Sichuan University, Chengdu, 610065, China

[f]Chongqing University Cancer Hospital, Chongqing University, Chongqing 400030, China

[g]Environmental Change Research Centre, University College London, Gower Street, London WC1E 6BT, United Kingdom

[*]Corresponding author: fengwenwang@cqu.edu.cn

Abstract:

Periodic water impoundment and seasonal flood events result in a 30 m water level fluctuation zone (WLFZ) in the Three Gorges Reservoir Region (TGRR), China.

In order to assess the occurrence, sources and seasonal variation of airborne carbonaceous pollutants, a total of thirty-nine $PM_{2.5}$ samples, twenty-two from August 2017 (summer: low water level ~135m) and seventeen from January 2018 (winter: high water level ~175m) were collected consecutively at a rural site in WLFZ in the TGRR. The results showed that OC, EC, char, soot, 16 PAHs and *n*-alkanes were higher in winter (mean: 9.17 μg/m^3, 4.69 μg/m^3, 4.25 μg/m^3, 0.45 μg/m^3, 19.8 ng/m^3 and 210 ng/m^3, respectively) than in summer (mean: 6.55 μg/m^3, 1.70 μg/m^3, 1.37 μg/m^3, 0.32 μg/m^3, 6.13 ng/m^3 and 79.1ng/m^3, respectively). Compositional differences suggested air-soil/plant exchange as a source for 2-3-rings PAHs in summer and biomass burning for 4-5-rings in winter. Diagnostic ratios and PCA suggested more vehicular emission for PAHs in summer. Plant waxes contributed 18.2 % and 26.2% of the *n*-alkanes in summer and winter, respectively, implying a relatively greater contribution from petroleum residues. The specific ratios and relative abundance of hopanes and steranes indicated mixed sources from both vehicle exhaust and petroleum residue; and petroleum residues contribute more steranes in summer compared with winter. As revealing basic information on the formation mechanism of carbonaceous aerosols, this study could contribute to a further understanding of their environmental geochemical behavior in the WLFZ of TGRR.

Keywords: carbonaceous pollutants; $PM_{2.5}$; seasonal variations; water level fluctuation zone; Three Gorges Reservoir

1 Introduction

Following construction of the Three Gorges Dam (TGD), one of the biggest

hydroelectric dams in the world (2309 m long and 181 m high), a prominent reservoir known as the Three Gorges Reservoir Region (TGRR), was formed on a main tributary of the Yangtze River of China (http://www.ctgpc.com.cn). As one key function of TGD is to produce electricity, the TGRR has been allowed to maintain low water levels from May to September and higher water levels from October to April, respectively. A water-level-fluctuation zone (WLFZ) that experiences a novel hydrological regime exposed during May to September (summer: minimum to ~145m water depth) and submerged at October to April (winter: maximum to ~175m water depth) in the TGRR was therefore formed (Zhang et al., 2008). As the TGRR has a length of ~190 km and an area of ~350 km^2, the WLFZ covers a large area and has given rise to environmental concerns since its complete impoundment in 2006. For example, Chen et al., (2009) compared the temporal-spatial CH_4 emissions among four vegetation stands in a typical drawdown area of WLFZ in 2008, finding important influence of water depth and dissolved organic carbon (DOC) on the spatial variations of emission flux and obvious seasonal variations with a maximal value in early July followed by a low and steady emission before winter flooding. Ye et al., (2011) assessed soil heavy metal pollution status before and after submergence across 12 sites in the WLFZ from 2008 to 2009, revealing that As and Cd were the primary pollutants before submergence; while afterwards, it was Hg, Cd, and Pb. Wang et al., (2013) investigated the distribution characteristics of USEPA priority 16 PAHs in the water of WLFZ between late-April and early-June 2011, showing that PAHs increased from town or counties to big industrialized cities and therefore could be used to trace

the water pollution status of TGR. Floehr et al., (2015) conducted a sampling campaign on sediments and fish at several sites of the WLFZ from 2011 to 2013 to determine organic pollution levels and mutagenic potential. High PAH occurrence was detected at sediments of two hot spots, Chongqing (150-433 ng/g) and Kaixian (127-590 ng/g), conforming their key role as major pollutant sources and sites of eco-toxicological risk in this area. Gao et al., (2017) reported the spatiotemporal variability of organotins (OTs) in surface water under different water levels from 2012 to 2013 along the TGRR, highlighting the significant role of dynamic water level conditions on the occurrence and compositions of OTs. Sang et al., (2019) evaluated the effects of water impoundment and water-level manipulation on heavy metals, finding apparent bioaccumulation of Cu, Fe, Zn and Hg in fish and aquatic invertebrates in high water levels (winter) of the TGRR. While these studies refer to the environmental behavior and ecological effects of major pollutants in the surface waters and sediments of the WLFZ, air-surface (water, soil and plant) exchange processes and fluxes of these pollutants could also be driven by the dynamic water level. However, to date, the variation in concentrations, compositions and sources of pollutants in the atmosphere between different seasons associated with water levels in the WLFZ have received little attention.

With a length of over 600 km and an area of 1,084 km^2, the TGRR extends from Jiangjin District of Chongqing Municipality to Yichang City of Hubei province (Chen et al., 2013). Approximately 80% area of the TGRR is under the jurisdiction of Chongqing Municipality. Chongqing, the largest city by population (over 30 million

in 2018), is one of the four municipalities and national financial and economic centers in southwest China. Due to rapid industrialization and urbanization, the $PM_{2.5}$ pollution in Chongqing has deteriorated in recent decades, especially with respect to the occurrence of atmospheric carbonaceous pollutants (e.g., Organic Carbon: OC and Elemental Carbon: EC) (Chow et al., 2006; Yang et al., 2011; Chen et al., 2014; Zhang et al., 2015). Influenced by the mountainous topography and unique meteorological conditions (low wind speeds, high frequency of temperature inversions) of the TGRR, these carbonaceous pollutants are readily trapped in the WLFZ following transport from Chongqing municipality and have a detrimental effect on its ecosystems (Wang et al., 2016b). Studying the variation of carbonaceous pollutants in $PM_{2.5}$ in different seasons could provide useful information on these pollutants and their formation mechanisms. However, to the best of our knowledge, there has been no report on the details of carbonaceous species in the atmosphere of WLFZ in TGRR. In this study, thirty-nine $PM_{2.5}$ samples, twenty-two from August 2017 (summer: low water level ~135m) and seventeen in January 2018 (winter: high water level ~175m), were collected consecutively at a rural site in a typical WLFZ of the TGRR. These samples were analyzed for carbonaceous pollutants, including OC, EC, char-EC (char), soot-EC (soot), 16 USEPA priority polycyclic aromatic hydrocarbons (16 PAHs), *n*-alkanes (26 species, C_{10}–C_{35}), as well as relative abundances of hopanes (10 species, C_{29}–C_{32}) and steranes (12 species, C_{27}–C_{29}). The purpose of this study was to assess the status of carbonaceous aerosol pollution in $PM_{2.5}$ driven by the dynamic water level and seasonal factors. This provides important

information on the formation mechanism of carbonaceous aerosols and could also contribute to a further understanding of their environmental geochemical behavior in the WLFZ of TGRR.

2 Materials and Methods

2.1 Sampling sites and sample collection

The sampling site (31º9′6″ N, 108º33′52″ E) is located at Pengxi River wetland nature reserve in TGRR (Figure 1). With low residential density and almost no industrial activity nearby, this nature reserve is about 30 km away from the center of Kaizhou district of Chongqing. The TGR water level in the reserve can reach ~175 m in January and drop to ~145 m in August, forming an area of 36 km^2 and a 30-m vertical drawdown zone in the wetlands. These features make this zone an ideal site to compare the characteristics of carbonaceous pollutants in the atmosphere between different seasons associated with water levels in TGRR.

The sampling apparatus was placed on the roof of a three-story building, 8 m away from a roof fence and 200 m above sea level. With an area of approximately 500 m^2, this sampling location is a ‘super’ scientific monitoring station affiliated to Chongqing Forestry Bureau and has been used previously by researchers to observe atmospheric deposition of polycyclic aromatic compounds (Tian et al., 2017) and inorganic nitrogen (NO_3^- and NH_4^+) (Wang et al., 2018). In this study, $PM_{2.5}$ samples were collected on quartz filters (20×25 cm^2, T2600, Pall Corporation, Port Washington, NY, USA) using a $PM_{2.5}$ sampler (ASM-1, Guangzhou Mingye Huanbao Technology Company, Guangzhou, China) at a flow rate of 300 L min^{-1}. Each sample

was based on 23.5-hours collection, starting at 09:00 and ending at 08:30 the following day. Two sampling campaigns, 22 Jul-13 Aug 2017 (summer, n=22, average temperature: 33°C) and 15 Jan-31 Jan 2018 (winter, n=17, average temperature: 8°C), were conducted to represent low and high water level, respectively. For each sampling period, we obtained two parallel operational sample blanks, which were collected by placing filters into the sampler without pumping air. Prior to sampling, the quartz filters were wrapped in aluminum foil and baked in a muffle furnace for 4 h at 450°C. The filters were then sealed in valve bags and stored in a desiccator. Following exposure, all samples including the operational blanks were stored at -20°C until further analysis. The filters were each divided into two halves. One was used for PAH and *n*-alkane analysis while the other half was used for EC and OC.

2.2 Sample analysis for OC and EC

A Thermal/Optical Carbon Analyzer (Desert Research Institute: DRI, Model 2015) was used to analyze OC and EC by IMPROVE thermal/optical reflectance (TOR) as suggested by Chow et al., (2007). For each sample, four OC fractions (OC1, OC2, OC3, and OC4), three EC fractions (EC1, EC2, and EC3) and a pyrolyzed carbon fraction (OP) were analyzed by taking areas of 0.544 cm^2 from the sampling filter. The OC fractions (1-4) were analyzed in a helium atmosphere at 140 °C, 280 °C, 480°C and 580 °C respectively. The EC fractions (1-3) were analyzed in a 2% oxygen/98% helium atmosphere at 580 °C, 740 °C and 840 °C, respectively. OP was used to monitor the charring of OC. OC is the sum of the four OC fractions plus OP. EC is the sum of the three EC fractions minus OP. Based on the identification of two

155 EC fractions provided by Han et al., (2009), char could be calculated as EC1 minus
156 OP and soot as the sum of EC2 and EC3.

157 **2.3 Sample analysis for PAHs, *n*-alkanes**

158 In order to extract PAHs and *n*-alkanes, dichloromethane (DCM) was used for
159 Soxhlet extraction lasting 48 hours. Before extraction, a known PAHs standard sample
160 consisting of deuterated naphthalene (Nap-d_8, m/z 136) (200 ng), deuterated
161 acenaphthene (Ace-d_{10}, m/z 164) (200 ng), deuterated phenanthrene (Phe-d_{10}, m/z 188)
162 (200 ng), deuterated chrysene (Chr-d_{12}, m/z 240) (200 ng) and deuterated perylene
163 (Per.$_{12}$, m/z 264) (200 ng) was added to DCM to monitor the efficiency of extraction.
164 After extraction, the mixed DCM was rotary evaporated to about 5 mL at 40°C and 50
165 rpm/min in a vacuum rotary evaporator. The extracts were transferred into 22 mL
166 glass bottles and evaporated down to about 2 mL by N_2 with a purity of 99%. The
167 concentrates were then purified on chromatography columns (8 mm in diameter, 20
168 cm in length), which, from bottom to top, were filled with 3 cm deactivated Al_2O_3, 3
169 cm SiO_2 and 1 cm Na_2SO_4. Subsequently, the columns were eluted three times with
170 20 mL dichloromethane/hexane (1:1, v: v). Before PAH analysis, the eluate was
171 further concentrated to about 500 μL under gentle N_2 stream.

172 The targeted PAHs were 16 USEPA priority PAHs. The following are the number
173 of rings, names and acronyms of these16 PAHs. 2-ring: naphthalene (Nap); 3-ring:
174 acenaphthylene (Ac), acenaphthene (Ace), fluorene (Fl), phenanthrene (Phe),
175 anthracene (Ant); 4-ring: fluoranthene (Flu), pyrene (Pyr), benzo[a]anthracene (BaA),
176 chrysene (Chr); 5-ring: benzo[b]fluoranthene (BbF), benzo[k]fluoranthene (BkF),

benzo[a]pyrene (BaP), dibenzo[a,h]anthracene (DBA); 6-ring: indeno[1,2,3-cd]pyrene (IP), benzo[ghi]perylene (BghiP). The molecular formulae of the 26 targeted *n*-alkanes are $C_{10}H_{22}$, $C_{11}H_{24}$, $C_{12}H_{26}$, $C_{13}H_{28}$, $C_{14}H_{30}$, $C_{15}H_{32}$, $C_{16}H_{34}$, $C_{17}H_{36}$, $C_{18}H_{38}$, $C_{19}H_{40}$, $C_{20}H_{42}$, $C_{21}H_{44}$, $C_{22}H_{46}$, $C_{23}H_{48}$, $C_{24}H_{50}$, $C_{25}H_{52}$, $C_{26}H_{54}$, $C_{27}H_{56}$, $C_{28}H_{58}$, $C_{29}H_{60}$, $C_{30}H_{62}$, $C_{31}H_{64}$, $C_{32}H_{66}$, $C_{33}H_{68}$, $C_{34}H_{70}$, $C_{35}H_{72}$.

For GC-MS analysis, hexamethylbenzene (HMB) was quantitatively (200ng) added to the samples as an internal standard. The GC-MSD (Agilent GC 6890 N coupled with 5975C MSD) was equipped with DB5-MS column (30 m × 0.25 mm × 0.25 μm) and highly purified helium (carrier gas, 99% in purity). The GC-MS operation is as follows: The temperature is set initially at 60°C for 2 min, further ramped to 290°C at 3 °C/min and held for 20 min. The samples were injected with the split-less mode at 290°C. The post-run time was 5 min at 310 °C.

Authentic standards of the 16 PAHs (Nap, Ac, Ace, Fl, Phe, Ant, Flu, Pyr, BaA, Chr, BbF, BkF, BaP, DBA, IP, BghiP) and 14 even numbered *n*-alkanes (C_{10}, C_{12}, C_{14}, C_{16}, C_{18}, C_{20}, C_{22}, C_{24}, C_{26}, C_{28}, C_{30}, C_{32}, C_{34} and C_{36}) were used to determine the concentration of PAHs and *n*-alkanes respectively. PAHs were quantified by the ions of m/z 128 for Nap, 152 for Ac, 153 for Ace, 166 for Fl, 178 for Phe and Ant, 202 for Pyr and Flu, 228 for BaA and Chr, 252 for BbF, BkF and BaP, 276 for IP and BghiP, 278 for DBA. *N*-alkanes were quantified by the ions at m/z 57 and 71. For the odd alkanes, we use the close even alkanes to calculate the abundance based on the retention times and mass spectra (Wang et al., 2017). The target component identification was based on the charge-mass ratio and retention times of the

chromatographic peaks with the standards.

2.3 Sample analysis for hopanes and steranes

The pretreatment process and GC-MS analysis of hopanes and steranes was the same as those for PAHs and *n*-alkanes. The 10 targeted hopanes and 12 steranes were detected by separating the characteristic ions: m/z 191 for hopanes, m/z 217 for 5α-, 14α- and 17α-steranes and m/z 218 for 5α-, 14β- and 17β-steranes. Without authentic standard samples (i.e., reference material) of the targeted hopanes and steranes, we still can present their relative abundances rather than concentration data. The abbreviation and forms of the 10 targeted hopanes and 12 steranes are shown in Table S1 in Supporting Information.

2.4 Quality Assurance / Quality Control (QA/QC)

The Thermal/Optical Carbon Analyzer was calibrated with known quantities of sucrose every day. One replicate analysis was performed for every 10 samples. The difference determined from replicate analyses was 3.0% for OC and EC, 4.5% for TC (total carbon) and 8.6% for char and soot. Results were corrected relative to the average blank concentrations.

The purity of organic solvent used in this study (DCM, Hexane) was 95% HPLC grade. Prior to pretreatment, all containers were soaked and washed with hot potassium dichromate and sulfuric acid immersion. These were then rinsed with de-ionized water (18.2 MΩ Milli-Q), wrapped in aluminum foil and baked at 450°C for 4 hours in a muffle furnace. Before use, all containers were rinsed three times with DCM.

For PAHs, the average surrogate recoveries were 63%±8% for Nap-d_8, 73%±5% for Ace-d_{10}, 91%±7% for Phe-d_{10}, 91%±4% for Chr-d_{12} and 94%±5% for Per-d_{12}, respectively. The reported PAHs concentrations were recovery corrected in this study. The QA/QC for *n*-alkanes was based on the recovery rate of Phe-d_{10} and Chr-d_{12} according to Guo et al., (2009). Nominal detection limits for individual PAHs ranged from 8 to 80 pg/m^3; and from 10 to 100 ng/m^3 for the 20 *n*-alkanes. Procedural blanks and standard-spiked blanks were analyzed and the results are within QA/QC requirements. Sample results were corrected by subtracting the average blank.

3 Results and discussion

3.1 Concentrations of OC, EC, char, soot, PAHs and *n*-alkanes

Table S2 in Supporting Information presents the eight fractions of OC, EC, 16 PAHs and 26 *n*-alkanes concentrations in all $PM_{2.5}$ samples. The average concentrations and some indices of carbonaceous pollutants in winter and summer are presented in Table 1. The average concentrations of OC (9.17 ± 5.03 μg/m^3) in winter were higher than those of summer (6.55 ± 2.27 μg/m^3). This difference was more apparent for EC, 4.69 ± 3.40 μg/m^3 in winter and 1.70 ± 0.71 μg/m^3 in summer, respectively. Similar results were observed for both char and soot: 4.25 ± 3.09 μg/m^3 for char and 0.45 ± 0.47 μg/m^3 for soot in winter and 1.37 ± 0.5 μg/m^3 for char and 0.32 ± 0.21 for soot in summer, respectively. Figure 2 shows the individual concentrations of OC, EC, char and soot in order to provide a better direct comparison. It could be seen that apart from soot, the differences between OC, EC and char are very similar and distinct during the sampling period. As regard PAHs and *n*-alkanes,

the average concentrations of PAHs was 19.8 ± 9.18 ng/m^3 in winter and 6.13 ± 1.27 ng/m^3 in summer; for *n*-alkanes, they were 210 ± 147 ng/m^3 and 79.1 ± 17.7 ng/m^3, respectively. These large differences indicate that there may be specific sources of high carbonaceous pollutants between summer and winter.

Table 2 provides a comparison of the carbonaceous pollutants, including OC, EC, char, soot, PAHs and *n*-alkanes in $PM_{2.5}$ measured in this study with other studies worldwide. The OC and EC concentrations in $PM_{2.5}$ at WLFZ (7.86 and 3.20 μg/m^3, respectively) were lower than a rural site at Shaanxi, China (38.1 and 4.91, respectively) (Zhu et al., 2012), comparable to background/rural sites at Dongguan, Lin'an and Haikou (Feng et al., 2015; Liu et al., 2017; Wang et al., 2015d), but higher than a remote site at Yulong mountain, China (1.84 and 0.55 μg/m^3, respectively) (Zhang et al., 2018) and a rural site at Simcoe, Canada (1.30 and 0.64 μg/m^3, respectively) (Jeong et al., 2013). With regard to char and soot, the concentrations of $PM_{2.5}$ at WLFZ (2.81 and 0.39 μg/m^3, respectively) were lower than a rural site in Shaanxi, China (4.05 and 0.86 μg/m^3, respectively) (Zhu et al., 2012), comparable to a rural site at Suthep Mountain in Chiangmai, Indochina (2.97 and 0.36 μg/m^3, respectively) (Chuang et al., 2013), but higher than at Qinghai Lake in China (0.16 and 0.22 μg/m^3, respectively) (Li et al., 2013). For PAHs and *n*-alkanes, the total concentrations of these two compounds in $PM_{2.5}$ at WLFZ (12.1 and 145 ng/m^3, respectively) were much higher than at Yulong mountain (0.97 and 6.53 ng/m^3, respectively) (Zhang et al., 2018), Qinghai Lake (0.69 and 6.47 ng/m^3, respectively) (Li et al., 2013), Singapore (0.76 and 25.5 ng/m^3, respectively) (Zhang et al., 2017)

and Qatar (0.56 and 8.53 ng/m^3, respectively) (Javed et al., 2019). However, at Lin'an, China, concentrations of PAHs were 26.9 ng/m^3 while *n*-alkanes concentrations were 62.2 ng/m^3 (Feng et al., 2015). These results demonstrate that the concentrations of *n*-alkanes in $PM_{2.5}$ at WLFZ of TGRR are up to ten times higher than those elsewhere (Table 2). It may be inferred that these *n*-alkanes may be derived from specific sources, such as epicuticular waxes, associated with higher plants in the TGRR.

3.2 SOC estimation and sources from OC/EC and char/soot ratios

EC is essentially a primary pollutant while OC is resulted from both primary emitted sources (primary organic carbon: POC) and secondary transformation from gaseous precursors (secondary organic carbon: SOC). When the OC/EC ratios exceed 2.0, the relationship of OC and EC can be used to estimate the SOC as (Turpin et al., 1995):

$$SOC = OC - POC$$

$$POC = EC \times (OC/EC)_{mim}$$

where $(OC/EC)_{min}$ is the the minimum ratio of OC/EC. This equation has been used by researchers to identify source categories and estimate levels of secondary organic carbon (SOC) (Chow et al., 1996; Castro et al., 1999; Cao et al., 2005; Feng et al., 2009). However, the ratio of char to soot (char/soot) may also be a valuable indicator to imply source variations since there are distinct changes between different emission sources (Han et al., 2010; Wang et al., 2019). Table 1 summarize the SOC concentrations, 2.47 ± 1.32 μg/m^3 in winter and 3.11 ± 2.00 μg/m^3 in summer, and

their relative contribution to OC (SOC/OC in %), 33.0 ± 22.3 in winter and 44.6 ± 22.2 in summer, respectively. Higher SOC concentrations (mean 3.11 μg/m^3) and SOC/OC (mean 44.6%) were observed in summer compared with winter, 2.47 μg/m^3 for SOC and 33.0% for SOC/EC, respectively. In summer, the air temperature could be as high as 40 °C with a high frequency of sunny days, generating more intense of solar radiation. Under these meteorological conditions, there could be much higher photochemical activity resulting in enhanced formation of SOC (Castro et al., 1999). In winter, the temperature fluctuated around 10 °C with a high frequency of rain, providing suitable meteorological conditions to preserve POC (Safai et al., 2014). As a consequence, carbonaceous pollutants could accumulate in the water and sediments of WLFZ in winter; while in summer, the conditions of high temperature, intensive solar radiation and oxygen availability in the exposed surface sediments could result in the re-emission of these carbonaceous pollutants to the atmosphere. Therefore, the difference between SOC and SOC/OC in $PM_{2.5}$ of WLFZ at TGRR between summer and winter could be due to the distinct seasonal meteorological conditions enhanced by air-water, air-sediment and air-plant exchange in this region.

Table 1 also presents the mean OC/EC and char/soot in $PM_{2.5}$ between winter and summer. The OC/EC was 2.47 ± 1.11 in winter and 4.24 ± 1.67 in summer, respectively. For char/soot, these were 14.3 ± 15.6 in winter and 4.69 ± 2.12 in summer, respectively, displaying a much more pronounced variation than OC/EC. According to Schauer et al., (2002) and Wang et al., (2015a), higher OC/EC (e.g., >4) are associated with wood/coal burning or SOC; while Saarikoski et al., (2008)

suggested that lower OC/EC (e.g., <4) could characterize the dominance of fossil-fuel burning sources, such as vehicle emissions. Therefore, the OC in $PM_{2.5}$ in summer could be from wood/coal burning and SOC; while EC was solely from wood/coal burning. Fossil-fuel combustion could be the main contributor to these two carbonaceous pollutants in winter. As regards char/soot, ratios of 0.60 for motor vehicle exhaust, 1.31 for coal combustion and 22.6 for biomass burning have been suggested by Chow et al., (2004); while ratios of >3 for biomass burning/coal combustion and <1.0 for motor vehicle exhausts were found by Han et al., (2010). The higher char/soot ratio in winter indicated dominance of biomass burning and could be associated with the burning of agricultural straw or firewood. In rural China, these materials are often burned in stoves for cooking and indoor heating in winter. The lower char/soot in summer indicates a major influence from fossil-fuel combustion, and could be explained by vehicle emissions as a result of intensive agricultural cultivation on the large exposed area of the WLFZ. Source identification from char/soot could be more reliable than that from OC/EC as it is not influenced by secondary organic formation processes and therefore will maintain the source fingerprints of the fuel type.

3.3 Compositions of PAHs and *n*-alkanes

Figure 3 shows the relative percentages of 16 PAHs and concentrations of 26 *n*-alkanes in $PM_{2.5}$ between winter and summer. Distinct differences in the percentages of Nap (2-ring), Phe, Ant (3-ring) and Flu, Pyr, BaA, Chr (4-ring) in total PAHs between these two seasons could be observed. In winter, Phe, Ant, Flu, Pyr,

BaA and Chr contributed 36.4% to the 16 PAHs; while in summer it was only 17.4%. BbF, BkF, BaA, DBA, IP, and BghiP (5~6-ring) dominated, and contributed 61.0% in winter and 74.0% in summer, respectively. Nap, Ac and Ace accounted for 2.21% in winter and 9.23% in summer, respectively. It has been reported that 4-ring PAHs are derived from both from coal combustion and biomass burning while 5-6-ring PAHs could originate from diesel and gasoline vehicle emissions (Harrison et al., 1996). Natural mineral dusts are also found to contain Nap, Ace, Fl, and Phe (Moon et al., 2008). The higher contribution from Nap, Ac and Ace in summer compared with winter indicates a possible "volatilization" from exposed surfaces (e.g., soils and plants) in WLFZ. The volatilization here was achieved by re-emission of aged PAHs from contaminated sediments that received high levels of pollutants during impoundment. Nap, Ac and Ace are emitted in the gaseous phase and then perhaps adsorbed onto $PM_{2.5}$ in the atmosphere (Wang et al., 2014). Further study that focuses on the air-soil/plant exchange of individual PAHs under different seasons associated with water levels are therefore needed and suggested. The higher contribution from Phe, Ant, Flu, Pyr, BaA and Chr in winter indicates organic pollutants emitted as a result of coal combustion and biomass burning such as agricultural straw or firewood.

The compositions of 26 *n*-alkanes (C_{10}-C_{35}) were similar between these two seasons. However, differences in their concentrations, especially for C_{25}-C_{33}, were clearly observed. In order to distinguish the biogenic and anthropogenic origins of *n*-alkanes, the carbon preference index (CPI) has been used to assess source information (Simoneit, 1986). The CPI in this study was calculated as the sum of the

353 concentrations of the odd carbon-number *(*e.g., C_{11}, C_{13}, C_{15}…*)* divided by the even
354 carbon-number (e.g., C_{10}, C_{12}, C_{14}…), i.e.: CPI= $\sum(C_{11}–C_{35})/\sum(C_{10}–C_{34})$. The CPI
355 was similar for the two seasons, averaging 1.24 ± 0.17 in winter and 1.27 ± 0.15 in
356 summer, respectively (Table 1). The CPI values around 1.00 were also observed at
357 TSP in a small town of Linzhi on the southeastern Tibetan Plateau, China (Chen et al.,
358 2014) and $PM_{2.5}$ of a remote island in East China Sea (Wang et al., 2015b). A CPI of
359 1.2 in $PM_{2.5}$ of December, 2011 in urban Shanghai, China was also presented by Wang
360 et al., (2016a). According to Simoneit, (1986), a CPI equivalent to 1.0 suggests a
361 dominance of sources from anthropogenic activity, such as gasoline
362 emissions/petroleum residues). Therefore, anthropogenic sources substantially
363 contributed to the *n*-alkanes in $PM_{2.5}$ of WLFZ in TGRR.

364 **3.4 Sources of PAHs and *n*-alkanes**

365 The molecular diagnostic ratios (MDRs), such as Phe/(Phe+Ant), Flu/(Flu+Pyr),
366 BaA/(BaA+Chr) and IP/(IP+BghiP), have been widely used to identify PAH sources
367 (Guo et al., 2009; Wang et al., 2014; Wang et al., 2015b). However, the use of these
368 ratios was based on a number of assumptions (Ravindra et al., 2008). First, each
369 emitting sources always release individual PAHs at the same ratios. Second, PAHs of
370 the same molecular weight have similar environmental fates, i.e., the concentration
371 ratio of PAH A against PAH B always remains constant during their entire
372 environmental lifespan. These assumptions make MDRs be useful tools especially on
373 the determination or speciation of the “fresh” emission sources around mixed
374 combustion sources such as urban atmosphere. Recently, Harrison, et al., (2018)

revealed the mechanism of distinct reactivity of PAHs during atmospheric transport and found OH and NO_3 radicals responsible for the gas phase oxidation of low molecular weight PAHs (fluoranthene and pyrene). Therefore, use of diagnostic ratios at remote locations could be misleading since there would be aged process associated with re-emission from re-suspended soil or plant surface. In this study, we combined MDRs with principal component analysis (PCA) to apportion the PAHs sources as to improve the ability of discrimination.

Figure 4 compares the Phe/(Phe+Ant), Flu/(Flu+Pyr), BaA/(BaA+Chr) and IP/(IP+BghiP) between summer and winter. Phe/(Phe+Ant) was 0.89 in winter and 0.92 in summer, indicating a dominant source from coal combustion/biomass burning. However, Flu/(Flu+Pyr) was 0.53 in winter and 0.48 in summer, respectively. This discrepancy suggests that, in winter, grass, wood, coal combustion dominated; while in summer fossil fuel combustion contributed the most. BaA/(BaA+Chr) was 0.36 in winter and 0.45 in summer, both characterizing vehicular emission. The values of IP/(IP+BghiP) in winter and summer were 0.54 and 0.62, respectively, indicating an origin from coal, wood and grass combustion.

PCA using SPSS 16.0 (SPSS Inc., Chicago, IL, USA) was performed on datasets containing eight MDRs PAHs (Phe, Ant, Flu, Pyr, BaA, Chr, IP, and BghiP). Table 3 presents two extracted PCs, PC1 and PC2, for both winter and summer. PCs explained 95.8% (53.2 and 42.6%, respectively) of the total variance for winter and 89.0% (62.1 and 26.9%, respectively) for summer. PC1 in winter had high loadings of Phe, Ant, Flu and Pyr, whereas PC1 in summer was dominated by Flu, Pyr, BaA, IP and BghiP.

Therefore, PC1 in winter was associated with coal combustion/biomass burning; PC1 in summer was more associated with vehicular emissions in addition with coal combustion/biomass burning (Harrison, et al., 1996; Rajput, et al., 2011; Wang et al., 2014). PC2 in winter had high loadings of IP and BghiP, whereas PC1 in summer was dominated by Phe and Ant. Hereby, PC2 in winter was characterized as vehicular emissions and PC2 in summer was assigned as crude oil leakage or refined petroleum release (Zakaria et al., 2002). The sources apportioned using these MDRs therefore complement each other, generating a more comprehensive understanding of the sources of $PM_{2.5}$-bound PAHs in WLFZ in TGRR.

Simoneit et al., (1991) suggested that the sources of *n*-alkanes could be mainly divided into plant waxes (natural) and petroleum residues (anthropogenic). The *n*-alkane with the highest concentration, namely C_{max}, was C_{26}-alkanes or C_{27}-alkanes in winter and C_{29}-alkanes or C_{31}-alkanes in summer, characterizing a source from epicuticular waxes of higher plants. Table 1 lists the relative contribution of plant waxes which was calculated as: Wax $C_n = [C_n-(C_{n+1}+C_{n-1})/2]/C_n$. The contribution from plant wax was 26.2 ± 13.6% in winter and 18.2 ± 8.90% in summer, respectively. In order to adapt to the periodic flooding conditions, the artificial cultured trees (e.g., Aeschynomene indica, Cyperus) could lose their leaves or these could be abraded, possibly emitting more epicuticular waxes to the atmosphere. In summer, there could be petroleum leakage due to fuel handling and/or refueling of the vehicles that undertake intensive agricultural cultivation on the exposed areas. The slight difference in percentage of plant waxes between the two seasons indicates that anthropogenic

activity contributes most of the total 26 $PM_{2.5}$-bound *n*-alkanes in WLFZ of TGRR. Actually, there have been some studies that also estimate the contribution from plant wax to total *n*-alkanes at other places. For example, as to the TSP samples that were collected from Lulang on the southeastern Tibetan Plateau, China, the percent of plant wax to total *n*-alkanes was higher in winter than that in summer, which was 27.9% and 18.5%, respectively (Chen et al., 2014). While in $PM_{2.5}$ of East China Sea, the percent of plant wax to total *n*-alkanes in winter was only 3.30% and in summer it was 9.00% (Wang et al., 2015a). With a CPI value of 1.2, a ratio of 8.20% from plant wax to total *n*-alkanes was observed in $PM_{2.5}$ of winter in urban Shanghai (Wang et al., 2016). These differences between these studies suggest spatial-temporal variations and uncertainties associated with the sample number and sampling apparatus and further research is required.

3.5 Relative abundances of hopanes, steranes, and their source implications

The ratios of Ts/Tm, αβC31 S/(S+R), and ααα C29 S/(S+R) are common parameters used to identify anthropogenic sources (Oros et al., 2000; Alves et al., 2008). As summarized in Table 1, Ts/Tm was 1.52 ± 0.36 in winter and 1.33 ± 0.48 in summer, respectively. αβC31 S/S+R was 0.57 ± 0.02 in winter and 0.57 ± 0.07 in summer. With regard to ααα C29 S/(S+R), it was 0.49 ± 0.08 in winter and 0.55 ± 0.06 in summer. According to Feng et al., (2005), a ratio of Ts/Tm < 1.0 indicates the influence of less thermally mature fuels (e.g., biomass and coal). Ts/Tm was >1.0 in both seasons, implying an impact from vehicle exhaust. The ratios of αβC31S/(S + R) both averaged 0.57, indicating a dominant source from traffic emissions (Fraser et al.,

1998). The αααC29 S/(S+R) was 0.49 ± 0.08 in winter and 0.55 ± 0.06 in summer. The relatively high αααC29 S/(S+R) suggests more mature petroleum residues in the atmosphere in summer (Zaghden et al., 2007), consistent with the suggestion of agricultural activity at this time.

The relative abundance diagrams of 10 hopanes and 12 steranes between summer and winter are shown in Figure 5. These abundances were calculated based on 18α(H)-22,29,30-trisnorneohopane (Ts: where Ts = 1) and C27-5α(H), 14α(H), 17α(H)-steranes (C27ααα(20S): where C27ααα(20S) = 1). It could be seen that the dominant hopanes in winter were C30αβ, followed by C29βα; while the dominant hopanes in summer were C30βα and C29βα. Non-catalytic converter equipped gasoline-powered vehicles could emit particle-bound C30αβ (Schauer et al., 2002). The dominant species of steranes during the two seasons were C29αββ(20S) and C29αββ(20R). These two species were found to be abundant in the particulate phase of non- catalytic converter equipped gasoline-powered vehicle tailpipes (Schauer et al., 2002). Similar patterns, namely C_{29} being more abundant than C_{28} and C_{27} steranes, was also found in surface sediments of the Bohai Sea, China, where it was attributed to crude oil leakage (Hu et al., 2009).

The ratios of Ts/Tm, αβC31 S/(S+R) (Table 1) and the relative abundance of hopanes (Figure 5) indicate mixed sources from vehicle exhaust and mature petroleum residues to the $PM_{2.5}$-bound hopanes in WLFZ of TGRR. The rations of αααC29 S/(S+R) (Table 1) and the relative abundance of steranes (Figure 5) also indicate vehicle exhaust and petroleum residues are the major sources of steranes and

463 petroleum residues contribute more of steranes in summer compared with winter.

464 **4 Conclusions**

465 This study provides the first datasets on the concentrations, sources and seasonal
466 variations of carbonaceous pollutants in $PM_{2.5}$ of two distinct water levels, ~175 m in
467 winter and 145 m in summer, at WLFZ of TGRR. All the carbonaceous pollutants had
468 higher concentrations in winter with respect to summer. The seasonal SOC and
469 SOC/OC ratio between summer and winter differs mainly as a result of distinct
470 air-water, air-soil and air-plant exchange in this region. The different compositions of
471 16 PAHs in the two sampling periods implies that the dominant sources were distinct,
472 with air-soil/plant exchange contributing 2~3-ring PAHs in summer and biomass
473 burning associated with agricultural straw or firewood contributing 4-5-ring PAHs in
474 winter. The results obtained by MDRs and source apportionment using PCA
475 complemented each other well, highlighting a prominent contribution from traffic
476 emissions to $PM_{2.5}$-bound PAHs in summer. The contribution of plant waxes to
477 *n*-alkanes in winter (26.2 ± 13.6%) was higher than that in summer (18.2 ± 8.90%),
478 possibly due to the loss or abrasion of leaves from trees (e.g., Aeschynomene indica,
479 Cyperus) under periodic flooding conditions. Petroleum residues are the dominant
480 source of steranes in summer, likely due to agricultural vehicles, while vehicle
481 exhaust was the most common source of hopanes and steranes in both seasons.

482 **Acknowledgement**

483 This work was funded by the National Natural Science Foundation of China
484 (NSFC) (No: 41603102), National Key R&D Program of China (No:

2018YFC0214003, 2019YFC1805500), the opening Project of Key Laboratory of Pollution Processes and Environmental Criteria, Ministry of Education (No: 201803), Technological Innovation and Application Development Key Projects of Chongqing Municipality, China (No: cstc2018jscx-mszdX0121). We would like to thank Mr. Shengdong Liu, Yong Cheng and Junnan Shi for the sample collection.

References

Alves, C.A., 2008. Characterisation of solvent extractable organic constituents in atmospheric particulate matter: an overview. Annals of the Brazilian Academy of Sciences, 80(1): 21-82.

Cao, J.J., Chow, J.C., Lee, S.C., Li, Y., Chen, S., An, Z.S., Fung, K., Watson, J., Zhu, C., Liu, S., 2005. Characterization and source apportionment of atmospheric organic and elemental carbon during fall and winter of 2003 in Xi'an, China. Atmos. Chem. Phys. 5, 3127-3137.

Castro, L., Pio, C., Harrison, R.M., Smith, D., 1999. Carbonaceous aerosol in urban and rural European atmospheres: estimation of secondary organic carbon concentrations. Atmos. Environ. 33, 2771-2781.

Chen, H., Wu, Y.Y., Yuan, X.Z., Gao, Y.H., Wu, N., Zhu, D., 2009. Methane emissions from newly created marshes in the drawdown area of the Three Gorges Reservoir. J. Geophys. Res. 114, D18301.

Chen, Y., Cao, J.J., Zhao, J., Xu, H.M., Arimoto, R., Wang, G.H., Han, Y.M., Shen, Z.X., Li, G.H., 2014. n-Alkanes and polycyclic aromatic hydrocarbons in total suspended particulates from the southeastern Tibetan Plateau: Concentrations,

seasonal variations, and sources. Sci. Total Environ. (470-471): 9-18.

Chen, Y., Xie, S.D., Luo, B., Zhai, C.Z., 2014. Characteristics and origins of carbonaceous aerosol in the Sichuan Basin, China. Atmos. Environ. 94, 215-223.

Chen, Z. B., Zhou, Z.Y., Peng, X., Xiang, H., Xiang, S.N., Jiang, Z.X., 2013. Effects of wet and dry seasons on the aquatic bacterial community structure of the Three Gorges Reservoir. World J. Microbiol. Biotechnol. 29, 841–853.

Chow, J.C., Watson, J., Lu, Z., Lowenthal, D., Frazier, C., Solomon, P., Thuillier, R., Maglinao, K., 1996. Descriptive analysis of $PM_{2.5}$ and PM_{10} at regionally representative locations during SJVAQS/AUSPEX. Atmos. Environ. 30, 2079-2112.

Chow, J.C., Watson, J.G., Kuhns, H.D., Etyemezian, V., Lowenthal, D.H., Crow, D.J., Kohl, S.D., Engelbrecht, J.P., Green, M.C., 2004. Source profiles for industrial, mobile, and area sources in the Big Bend regional aerosol visibility and observational (BRAVO) study. Chemosphere. 54, 185-208.

Chow, J.C., Watson, J.G., Chen, L-W., A., Ho, S.S., Koracin, D., Zielinska, B., Tang, D.L., Perera, F., Cao, J.J., Lee, S.C., 2006. Exposure to $PM_{2.5}$ and PAHs from the Tong Liang,China epidemiological study. J. Environ. Sci. Health., Part A. 41 (4), 517-542.

Chow, J.C., Watson, J.G., Chen, L-W., A., Chang, M.C.O., Robinson, N.F., Trimble, D., Kohl, S., 2007. The IMPROVE_A Temperature Protocol for Thermal/Optical Carbon Analysis: Maintaining Consistency with a Long-Term Database. J. Air & Waste Manage. Assoc., 57: 9, 1014-1023.

529 Chuang, M.T., Chou, C.K., Sopajaree, K., Lin, N.H., Wang, J.L., Sheu, G.R., Chang,
530 Y.J., Lee, C.T., 2013. Characterization of aerosol chemical properties from
531 near-source biomass burning in the northern Indochina during 7-SEAS/Dongsha
532 experiment. Atmos. Environ. 78 (Sp. Iss. SI), 72-81.
533 Feng, J.L., Chan, C.K., Fang, M., Hu, M., He, L.Y., Tang, X.Y., 2005. Impact of
534 meteorology and energy structure on solvent extractable organic compounds of
535 $PM_{2.5}$ in Beijing, China. Chemosphere. 61, 623-632.
536 Feng, J.L, Hu, J.C., B. Xu, B.H., Hu, X.L., Sun, P., Han, W.L., Gu, Z.P., Yu, X.M., Wu,
537 M.H., 2015. Characteristics and seasonal variation of organic matter in $PM_{2.5}$ at a
538 regional background site of the Yangtze River Delta region, China. Atmos.
539 Environ. 123, 288-297.
540 Feng, Y.L., Chen, Y.J., Guo, H.Z., Li, J., Sheng, G.Y., Fu, J.M., 2009. Characteristics
541 of organic and elemental carbon in $PM_{2.5}$ samples in Shanghai, China. Atmos.
542 Res. 92, 0-442.
543 Floehr, T., Scholz-Starke, B., Xiao, H.X., Koch, J., Wu, L.L., Hou, J.L., Wolf, A.,
544 Bergmann, A., Bluhm, K., Yuan, X.Z., Roß-Nickoll, M., Schäffer, A., Hollert, H.,
545 2015. Yangtze Three Gorges Reservoir, China: a holistic assessment of organic
546 pollution, mutagenic effects of sediments and genotoxic impacts on fish. J.
547 Environ. Sci. 38, 63-82.
548 Fraser, M., Cass, G., Simoneit, B., 1998. Gas-Phase and particle-phase organic
549 compounds emitted from motor vehicle traffic in a Los Angeles roadway tunnel.
550 Environ. Sci. Technol. 32, 2051-2060.

551 Gao, J.M., Wu, L., Chen, Y.P., Zhou, B., Guo, J.S., Zhang, K., Ouyang, W.J., 2017.
552 Spatiotemporal distribution and risk assessment of organotins in the surface
553 water of the Three Gorges Reservoir Region, China. Chemosphere. 171,
554 405-414.
555 Guo, Z.G., Lin, T., Zhang, G., Hu, L.M., Zheng, M., 2009. Occurrence and sources of
556 polycyclic aromatic hydrocarbons and n-alkanes in PM2.5 in the roadside
557 environment of a major city in China. J. Hazard. Mater. 170, 888-894.
558 Han, Y. M., Lee, S. C., Cao, J. J., Ho, K. F., and An, Z. S., 2009. Spatial distribution
559 and seasonal variation of char-EC and soot-EC in the atmosphere over China.
560 Atmos. Environ. 43, 6066–6073.
561 Han, Y.M., Cao, J.J., Lee, S.C., Ho, K.F., An, Z.S., 2010. Different characteristics of
562 char and soot in the atmosphere and their ratio as an indicator for source
563 identification in Xi'an, China. Atmos. Chem. Phys. 10, 595-607.
564 Harrison, R., Smith, D., Luhana, L., 1996. Source apportionment of atmospheric
565 polycyclic aromatic hydrocarbons collected from an urban location in
566 Birmingham, UK. Environ. Sci. Technol. 30, 825-832.
567 Harrison, R.M., Yin, J., 2010. Chemical speciation of $PM_{2.5}$ particles at urban
568 background and rural sites in the UK atmosphere. J Environ Monit. 12,
569 1404-1414.
570 Harrison, R.M., Jang, E., Alam, M.S., Dang, J., 2018. Mechanisms of reactivity of
571 benzo(a)pyrene and other PAH inferred from field measurements. Atmos. Pollut.
572 Res., 9 (6), 1214-1220.

573 Javed, W., Iakovides, M., Stephanou, E.G., Wolfson, J.M., Koutrakis, P., Guo, B.,
574 2019. Concentrations of aliphatic and polycyclic aromatic hydrocarbons in
575 ambient $PM_{2.5}$ and PM_{10} particulates in Doha, Qatar. J. Air Waste Manage. Assoc.
576 69 (2), 162-177.
577 Jeong, C.H., Herod, D., Dabek-Zlotorzynska, E., Ding, L.Y., McGuire, M.L., Evans,
578 G., 2013. Identification of the Sources and Geographic Origins of Black Carbon
579 using Factor Analysis at Paired Rural and Urban sites. Environ. Sci. Technol. 47
580 (15), 8462-8470.
581 Katsoyiannis, A., Breivik, K., 2014. Model-based evaluation of the use of polycyclic
582 aromatic hydrocarbons molecular diagnostic ratios as a source identification tool.
583 Environ. Pollut. 184: 488-494.
584 Li, J.J., Wang, G.H., Wang, X.M., Cao, J.J., Sun, T., Cheng, C.L., Meng, J.J., Hu, T.F.,
585 Liu, S.X., 2013. Abundance, composition and source of atmospheric $PM_{2.5}$ at a
586 remote site in the Tibetan Plateau, China. Tellus B. 65, 20281.
587 Lim, S., Lee, M., Lee, G., Kim, S., Yoon, S., Kang, K., 2012. Ionic and carbonaceous
588 compositions of PM_{10}, $PM_{2.5}$ and $PM_{1.0}$ at Gosan ABC Superstation and their
589 ratios as source signature. Atmos. Chem. Phys. 12(4), 2007-2024.
590 Liu, B.S., Zhang, J.Y., Wang, L., Liang, D.N., Cheng, Y., Wu, J.H., Bi, X.H., Feng,
591 Y.C., Zhang, Y.F., Yang, H.H., 2018. Characteristics and sources of the fine
592 carbonaceous aerosols in Haikou, China. Atmos. Res. 199, 103-112.
593 Moon, K.J., Han, J.S., Ghim, Y.S., Kim, Y.J., 2008. Source apportionment of fine
594 carbonaceous particles by positive matrix factorization at Gosan background site

595 in East Asia. Environ. Int. 34, 654-664.

596 Oros, D.R., Simoneit, B.R.T., 2000. Identification and emission rates of molecular
597 tracers in coal smoke particulate matter. Fuel. 79, 515-536.

598 Rajput, P., Sarin, M., Rengarajan, R., Singh, D., 2011. Atmospheric polycyclic
599 aromatic hydrocarbons (PAHs) from post-harvest biomass burning emissions in
600 the Indo-Gangetic Plain: Isomer ratios and temporal trends. Atmos. Environ. 45,
601 6732-6740.

602 Ravindra, K., Sokhi, R., Grieken, R.V., 2008. Atmospheric polycyclic aromatic
603 hydrocarbons: Source attribution, emission factors and regulation. Atmos.
604 Environ. 42, 2895-2921.

605 Saarikoski, S., Timonen, H., Saarnio, K., Aurela, M., Jarvi, L., Keronen, P., Kerminen,
606 V.-M., Hillamo, R., 2008. Sources of organic carbon in fine particulate matter in
607 northern European urban air. Atmos. Chem. Phys. 8, 6281-6295.

608 Sang, C., Zheng, Y.Y., Zhou, Q., Li, D.P., Liang, G.D., Gao, Y.W., 2019. Effects of
609 water impoundment and water-level manipulation on the bioaccumulation
610 pattern, trophic transfer and health risk of heavy metals in the food web of Three
611 Gorges Reservoir (China). Chemosphere. 232, 403-414.

612 Safai, P.D., Raju, M.P., Rao, P.S.P., Pandithurai, G., 2014. Characterization of
613 carbonaceous aerosols over the urban tropical location and a new approach to
614 evaluate their climatic importance. Atmos. Environ. 92, 493-500.

615 Schauer, J.J., Kleeman, M.J., Cass, G.R., Simoneit, B.R.T., 2002. Measurement of
616 emissions from air pollution sources. 5. C_1-C_{32} organic compounds from

gasoline-powered motor vehicles. Environ. Sci. Technol. 36, 1169-1180.

Simcik, M., Eisenreich, S., Lioy, P., 1999. Source apportionment and source/sink relationships of PAHs in the coastal atmosphere of Chicago and Lake Michigan. Atmos. Environ. 33, 5071-5079.

Simoneit, B.R.T., 1986. Characterization of organic constituents in aerosols in relation to their origin and transport: a review. Inter. J. Environ. Ana. Chem. 23, 207-237.

Simoneit, B.R.T., Sheng, G.Y., Chen, X.J., Fu, J.M., Zhang, J., Xu, Y.P., 1991. Molecular marker study of extractable organic matter in aerosols from urban areas of China. Atmos. Environ. 25, 2111-2129.

Tian, M., Yang, F.M., Chen, S.J., Wang, H.B., Chen, Y., Zhang, L.Y., Zhang, L.M., Xiang, L., Qiao, B.Q., 2017. Atmospheric deposition of polycyclic aromatic compounds and associated sources in an urban and a rural area of Chongqing, China. Chemosphere. 187, 78-87.

Turpin, B., Huntzicker, J., 1995. Identification of secondary organic aerosol episodes and quantitation of primary and secondary organic aerosol concentrations during SCAQS. Atmos. Environ. 29, 3527-3544.

Wang, F.W., Lin, T., Li, Y.Y., Ji, T.Y., Ma, C.L., Guo, Z.G., 2014. Sources of polycyclic aromatic hydrocarbons in $PM_{2.5}$ over the East China Sea, a downwind domain of East Asian continental outflow. Atmos. Environ. 92, 484-492.

Wang, F.W., Guo, Z.G., Lin, T., Hu, L.M., Chen, Y.J., Zhu, Y.F., 2015a. Characterization of carbonaceous aerosols over the East China Sea: The impact of the East Asian continental outflow. Atmos. Environ. 110, 163-173.

639 Wang, F.W., lin, T., Feng, J.L., Fu, H.Y., Guo, Z.G., 2015b. Source apportionment of
640 polycyclic aromatic hydrocarbons in $PM_{2.5}$ using positive matrix factorization
641 modeling in Shanghai, China. Environ. Sci.: Processes Impacts, 17, 197-205.
642 Wang, F.W., Guo, Z.G., Lin, T., Rose, N.L., 2016a. Seasonal variation of
643 carbonaceous pollutants in $PM_{2.5}$ at an urban 'supersite' in Shanghai, China.
644 Chemosphere, 146, 238-244.
645 Wang, F.W., Lin, T., Li, Y.Y., Guo, Z.G., Rose, N.L., 2017. Comparison of $PM_{2.5}$
646 carbonaceous pollutants between an urban site in Shanghai and a background site
647 in a coastal East China Sea island in summer: concentration, composition and
648 sources. Environ. Sci.: Processes Impacts, 19, 833-842.
649 Wang, F.W., Feng, T., Guo, Z.G., Li, Y.Y., Lin, T., Rose, N.L., 2019. Sources and dry
650 deposition of carbonaceous aerosols over the coastal East China Sea:
651 Implications for anthropogenic pollutant pathways and deposition. Environ.
652 Pollut. 245, 771-779.
653 Wang, H.B., Shi, G.M., Tian, M., Chen, Y., Qiao, B.Q., Zhang, L.Y., Yang, F.M.,
654 Zhang, L.M., Luo, Q., 2018. Wet deposition and sources of inorganic nitrogen in
655 the Three Gorges Reservoir Region, China. Environ. Pollut. 233, 520-528.
656 Wang, J.Z., Ho S.S.H., Cao, J.J., Huang, R.J., Zhou, J.M., Zhao, Y.H., Xu,H.M., Liu,
657 S.X., Wang G.H., Shen, Z.Z., Han, Y.M., 2015c. Characteristics and major
658 sources of carbonaceous aerosols in $PM_{2.5}$ from Sanya, China. Sci. Total Environ.
659 530-531, 110-119.
660 Wang, J.X., Henkelmann, B., Bi, Y.H., Zhu, K.X., Pfister, G., Hu, W., Temoka, C.,

Westrich, B., Schramm, K.W., 2013. Temporal variation and spatial distribution of PAH in water of Three Gorges Reservoir during the complete impoundment period. Environ. Sci. Pollut. Res. 20, 7071-7079.

Wang, J.X., Bi, Y.H., Henkelmann, B., Pfister, G., Zhang, L., Schramm, K.W., 2016b. PAHs and PCBs accumulated by SPMD-based virtual organisms and feral fish in Three Gorges Reservoir, China. Sci. Total Environ. 542, 899-907.

Wang, Q.Q., Huang, X.H.H., Zhang, T., Zhang, Q.Y., Feng, Y.M., Yuan, Z.B., Wu, D., Lau, A.K.H., Yu, J.Z., 2015d. Organic tracer-based source analysis of $PM_{2.5}$ organic and elemental carbon: A case study at Dongguan in the Pearl River Delta, China. Atmos. Environ. 118, 164-175.

Yang, F., Tan, J., Zhao, Q., Du, Z., He, K., Ma, Y., Duan, F., Chen, G., Zhao, Q., 2011. Characteristics of $PM_{2.5}$ speciation in representative megacities and across China. Atmos. Chem. Phys. 11 (11), 5207-5219.

Ye, C., Li, S.Y., Zhang, Y.L., Zhang, Q.F., 2011. Assessing soil heavy metal pollution in the water-level-fluctuation zone of the Three Gorges Reservoir, China. J. Hazard. Mater. 191, 366-372.

Yunker, M., Macdonald, R., Vingarzan, R., Mitchell, R., Goyette, D.H., Sylvestre, S., 2002. PAHs in the Fraser River basin: a critical appraisal of PAH ratios as indicators of PAH source and composition. Org. Geochem. 33, 489-515.

Zaghden, H., Kallel, M., Elleuch, B., Oudot, J., Saliot, A., 2007. Sources and distribution of aliphatic and polyaromatic hydrocarbons in sediments of Sfax, Tunisia, Mediterranean Sea. Mar. Chem. 105, 70-89.

683 Zakaria, M., Takada, H., Tsutsumi, S., Ohno, K., Yamada, J., Kouno, E., Kumata, H.,
684 2002. Distribution of polycyclic aromatic hydrocarbons (PAHs) in rivers and
685 estuaries in Malaysia: a widespread input of petrogenic PAHs. Environ. Sci.
686 Technol. 36, 1907-1918.
687 Zhang, H., 2008. Characteristic analyses of the water-level-fluctuating zone in the
688 Three Gorges Reservoir. Bull. Soil Water Conserv. 28, 46-49. (In Chinese)
689 Zhang, L.Y., Huang, Y.M., Liu, Y., Yang, F.M., Lan, G.X., Fu, C., Wang, J., 2015.
690 Characteristics of Carbonaceous Species in $PM_{2.5}$ in Wanzhou in the Hinterland
691 of the Three Gorges Reservior of Northeast Chongqing, China. Atmosphere. 6,
692 534-546.
693 Zhang, N.N., Cao, J.J., Wang, Q.Y., Huang, R.J., Zhu, C.S., Xiao, S., Wang, L.L.,
694 2018. Biomass burning influences determination based on $PM_{2.5}$ chemical
695 composition combined with fire counts at southeastern Tibetan Plateau during
696 pre-monsoon period. Atmos. Res. 206, 108-116.
697 Zhang, Z.H., Khlystov, A., Norford, L.K., Tan, Z.K., Balasubramanian, R., 2017.
698 Characterization of traffic-related ambient fine particulate matter ($PM_{2.5}$) in an
699 Asian city: Environmental and health implications. Atmos. Environ. 161,
700 132-143.
701 Zhu, C.S., Cao, J.J., Shen, Z.X., Liu, S.X., Zhang, T., Zhao, Z.Z., Xu, H.M., Zhang,
702 E.K., 2012. Indoor and Outdoor Chemical Components of $PM_{2.5}$ in the Rural
703 Areas of Northwestern China. Aerosol Air Qual. Res. 12 (6), 1157-1165.
704

Table captions

Table 1 Concentrations and some indices of carbonaceous pollutants in $PM_{2.5}$ between summer and winter in WLFZ (n=22 and 17 in summer and winter, respectively, average ± stdev).

Table 2 Comparisons of the carbonaceous pollutants in $PM_{2.5}$ measured this study with other places worldwide (OC, EC, Char, Soot in μg/m^3, PAHs and *n*-alkanes in ng /m^3).

Table 3 Correlation factor loading matrix of selected eight PAHs in $PM_{2.5}$ (" - " indicate values of the factor loading below zero).

Figure captions

Figure 1 Sampling site at WLFZ of TGRR.

Figure 2 Comparisons of OC, EC, char and soot in $PM_{2.5}$ between summer and winter associated with water levels.

Figure 3 The compositions of PAHs and *n*-alkanes in $PM_{2.5}$ between summer and winter.

Figure 4 The diagnostic ratios of Phe/(Phe+Ant), Flu/(Flu+Pyr), BaA/(BaA+Chr) and IP/(IP+BghiP) of $PM_{2.5}$ between summer and winter.

Figure 5 Abundance distribution diagrams of relative hopane and sterane of $PM_{2.5}$ between summer and winter.

(Ts:18α(H)-22,29,30-trisnorneohopane;Tm:17α(H)-22,29,30-trisnorhopane;C_{29}αβ:17α(H),21β(H)-norhopane;C_{29}βα:17β(H),21α(H)-norhopane;C_{30}αβ:17α(H),21β(H)-hopane;C_{30}βα:17β(H),21α(H)-hopane;C_{31}S:22S-17α(H),21β(H)-homohopane;C_{31}R:22R-17α(H),21β(H)-homoho

pane;C_{32}S:22S-17α(H),21β(H)-bishomohopane;C_{32}R:22R-17α(H),21β(H)-bishomohopane)

(C27ααα(20S), C27αββ(20R), C27αββ(20S), C27ααα(20R), C28ααα(20S), C28αββ(20R),

C28αββ(20S), C28ααα(20R), C29ααα(20S), C29αββ(20R), C29αββ(20S), C29ααα(20R), and

ααα = 5α(H), 14α(H), 17α(H)-steranes; αββ = 5α(H), 14β(H), 17β(H)-steranes, R and S =

C-20 R and S configuration, respectively.)

Table 1 Concentrations and some indices of carbonaceous pollutants in $PM_{2.5}$ between summer and winter in WLFZ (n=22 and 17 in summer and winter, respectively, average ± stdev).

Sampling period	Seasons (water level)	OC	EC	SOC	Char	Soot	OC/EC	Char/Soot	SOC/OC (%)
		μg/m^3							
2017/07/22-08/25	summer (145 m)	6.55±2.27	1.70±0.71	3.11±2.00	1.37±0.57	0.32±0.21	4.24±1.67	4.69±2.12	44.6±22.2
2018/01/15-01/31	winter (175 m)	9.17±5.03	4.69±3.40	2.47±1.32	4.25±3.09	0.45±0.47	2.47±1.11	14.3±15.6	33.0±22.3
		16 PAHs	*n*-alkanes (C_{10}-C_{35}, 26 species)				hopanes		steranes
		ng/m^3	yield (ng/m^3)	CPI	C_{max}	waxed (%)	Ts/Tm	αβC31 S/S+R	ααC29 S/S+R
2017/07/22-08/25	summer (145 m)	6.13±1.27	79.1±17.7	1.27±0.15	C_{29}/C_{31}	18.2±8.90	1.33±0.48	0.57±0.07	0.55±0.06
2018/01/15-01/31	winter (175 m)	19.8±9.18	210±147	1.24±0.17	C_{26}/C_{27}	26.2±13.6	1.52±0.36	0.57±0.02	0.49±0.08

Table 2 Comparisons of the carbonaceous pollutants in $PM_{2.5}$ measured this study with other places worldwide (OC, EC, Char, Soot in μg/m^3, PAHs and *n*-alkanes in ng /m^3).

Location	Type of site	Time	Sample number	OC	EC	Char	Soot	ΣPAHs	Σ*n*-alkanes	Reference
WLFZ in TGRR	rural	Jul., 2017-Jan., 2018	n=39	7.86	3.20	2.81	0.39	12.1	145	This study
Sanya, China	suburban	Jan., 2012-Jul., 2013	n=42	3.30	1.10	0.95	0.15	6.85	14.8	Wang et al. (2015c)
Dongguan, China	rural	Feb.,2010-Dec., 2012	n=156	10.4	2.68	-	-	8.97	44.7	Wang et al. (2015d)
Shaanxi, China	rural	Nov., 2007-Dec., 2008	n=53	38.1	4.91	4.05	0.86	-	-	Zhu et al. (2012)
Lin'an, China	background	Apr., 2008-Jan., 2009	n=110	10.3	1.54	-	-	26.9	62.2	Feng et al. (2015)
Haikou, China	background	Jan., 2015-Sep., 2015	-	5.70	2.40	2.10	0.30	-	-	Liu et al. (2017)
Mt. Yulong, China	remote	Mar., 2012-Apr., 2012	n=30	1.84	0.55	-	-	0.97	6.53	Zhang et al. (2018)
Qinghai Lake, China	remote	Jul., 2010-Aug., 2010	n=56	1.58	0.37	0.16	0.22	0.69	6.47	Li et al. (2013)
Singapore	background	Nov., 2015-Feb., 2016	n=24	3.49	1.06	-	-	0.76	25.5	Zhang et al. (2017)
Simcoe, Canada	rural	Feb., 2005-Nov., 2007	n=143	1.30	0.64	0.07	0.57	-	-	Jeong et al. (2013)

West Midlands, UK	rural	May., 2007-Apr., 2008	n=60	2.50	1.10	-	-	1.49	23.4	Harrison et al. (2010)
Chiangmai, Indochina	rural	Mar., 2010-Apr., 2010	n=15	18.6	3.33	2.97	0.36	-	-	Chuang et al. (2013)
Doha, Qatar	suburban	May. 2015-Dec., 2015.	n=105	1.78	2.61	-	-	0.56	8.53	Javed et al. (2019)
Jeju Island, South Korea	coastal	Aug., 2007-Sep., 2008	n=41	4.00	1.70	1.30	0.40	-	-	Lim et al. (2012)

Table 3 Correlation factor loading matrix of selected eight PAHs in $PM_{2.5}$ (" - " indicate values of the factor loading below zero).

$PM_{2.5}$		winter		summer	
8 species		PC1	PC2	PC1	PC2
PAHs	Phe	0.979	0.120	-	0.721
	Ant	0.791	0.442	0.007	0.821
	Flu	0.911	0.386	0.927	0.064
	Pyr	0.849	0.508	0.958	0.001
	BaA	0.668	0.720	0.939	-
	Chr	0.722	0.668	0.741	-
	IP	0.288	0.952	0.961	-
	BghiP	0.263	0.960	0.908	-
	explained variance %	53.2	42.6	62.1	26.9

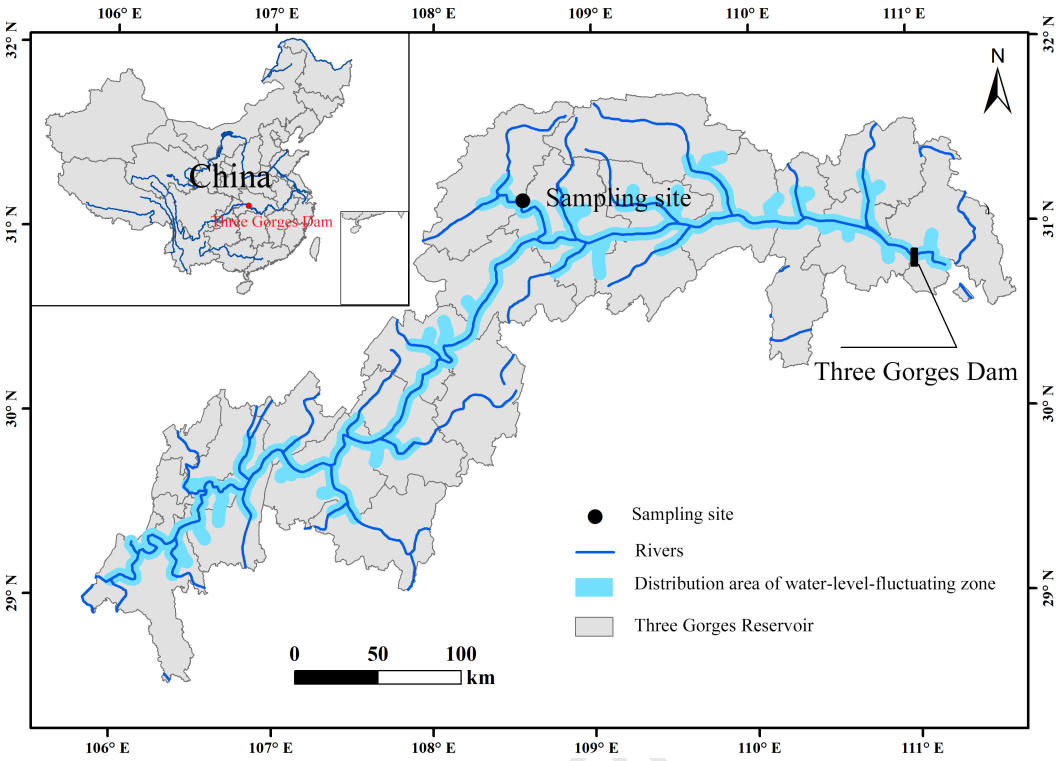

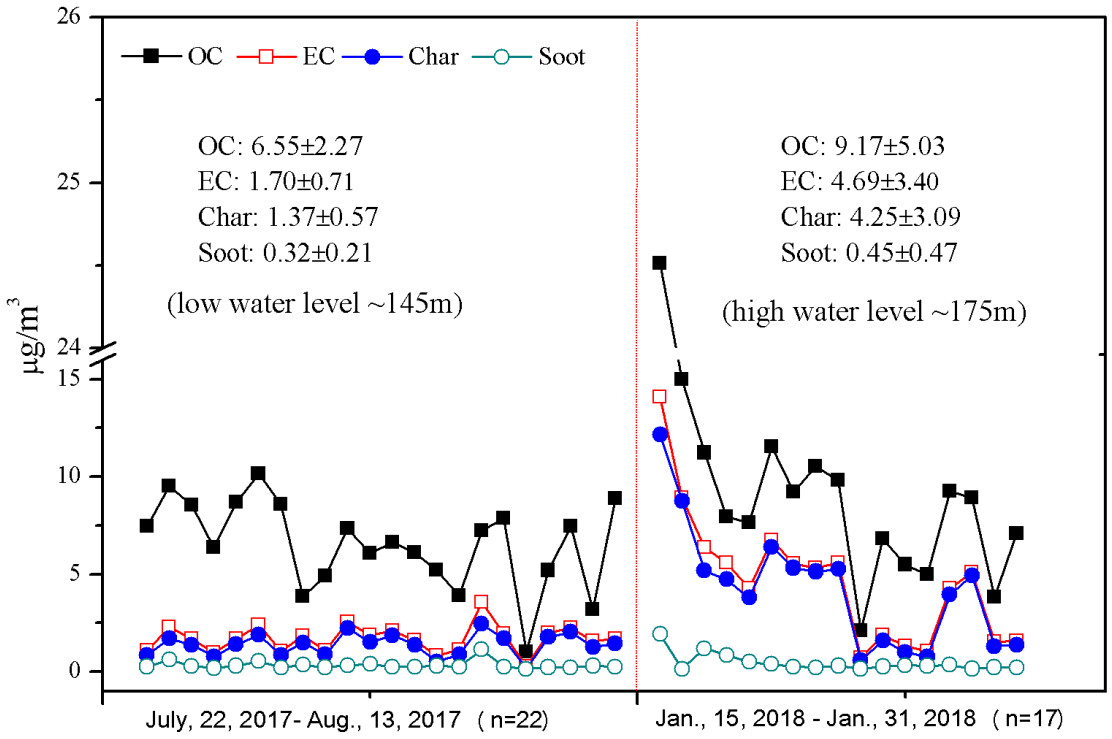
OC
EC
Char
Soot
OC: 6.55±2.27
EC: 1.70±0.71
Char: 1.37±0.57
Soot: 0.32±0.21
(low water level ~145m)
OC: 9.17±5.03
EC: 4.69±3.40
Char: 4.25±3.09
Soot: 0.45±0.47
(high water level ~175m)
μg/m3
July, 22, 2017- Aug., 13, 2017 (n=22)
Jan., 15, 2018 - Jan., 31, 2018 (n=17)

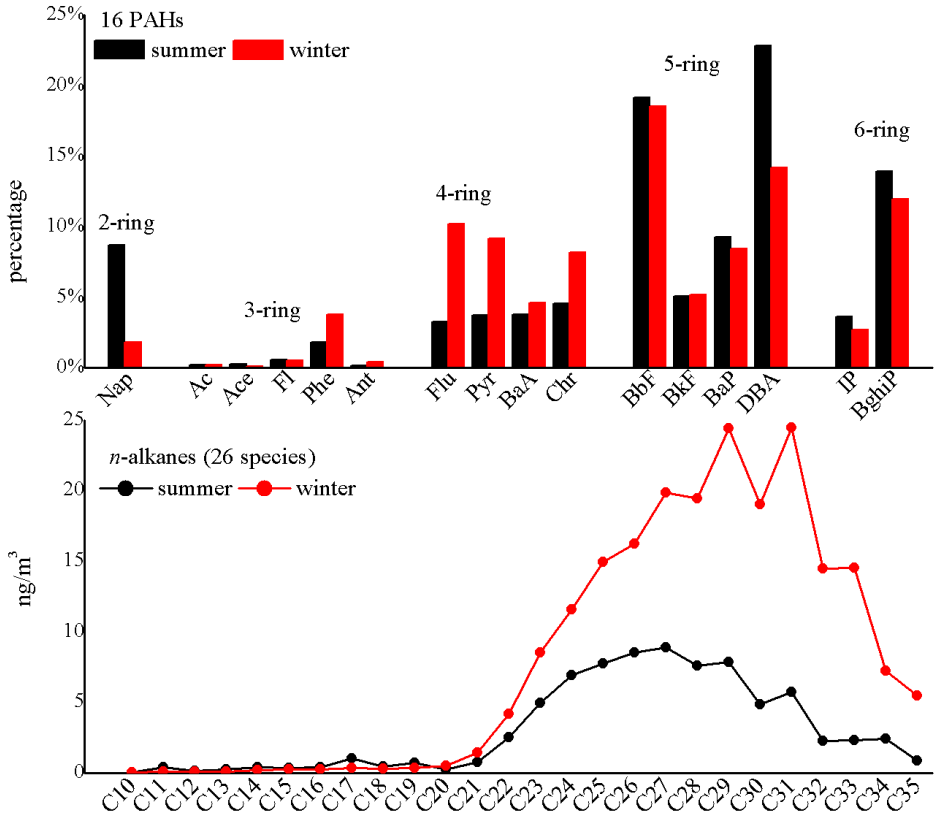
16 PAHs
summer
winter
percentage
25%
20%
15%
10%
5%
0%
2-ring
3-ring
4-ring
5-ring
6-ring
Nap
Ac
Ace
Fl
Phe
Ant
Flu
Pyr
BaA
Chr
BbF
BkF
BaP
DBA
IP
BghiP
n-alkanes (26 species)
summer
winter
ng/m3
25
20
15
10
5
0
C10
C11
C12
C13
C14
C15
C16
C17
C18
C19
C20
C21
C22
C23
C24
C25
C26
C27
C28
C29
C30
C31
C32
C33
C34
C35

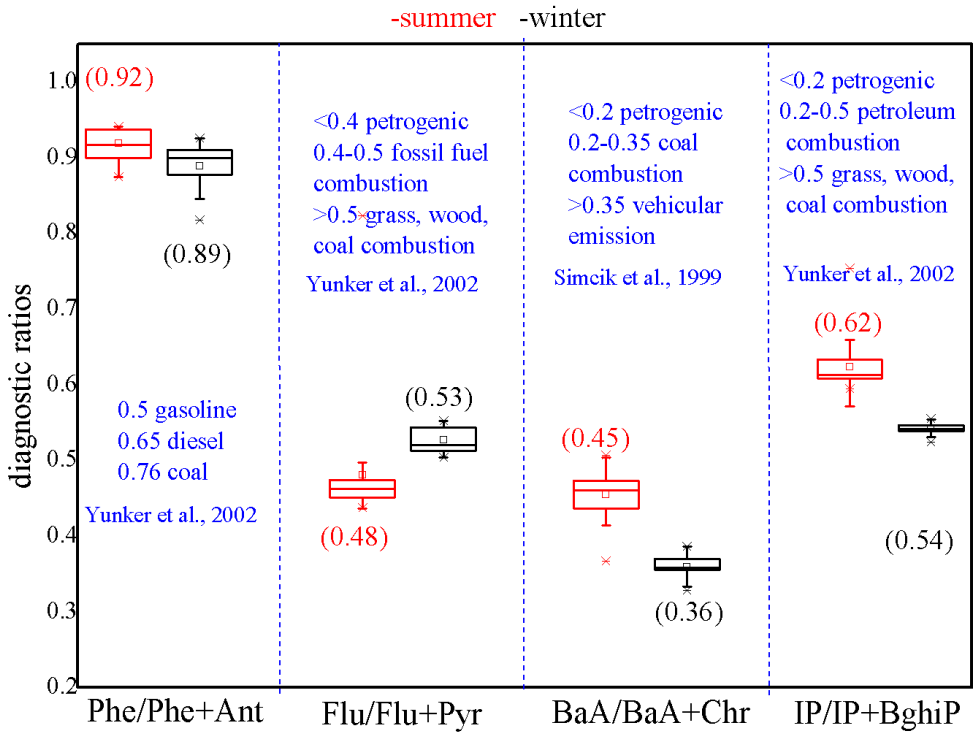
-summer -winter
diagnostic ratios
1.0
0.9
0.8
0.7
0.6
0.5
0.4
0.3
0.2
(0.92)
(0.89)
0.5 gasoline
0.65 diesel
0.76 coal
Yunker et al., 2002
<0.4 petrogenic
0.4-0.5 fossil fuel combustion
>0.5 grass, wood, coal combustion
Yunker et al., 2002
(0.53)
(0.48)
<0.2 petrogenic
0.2-0.35 coal combustion
>0.35 vehicular emission
Simcik et al., 1999
(0.45)
(0.36)
<0.2 petrogenic
0.2-0.5 petroleum combustion
>0.5 grass, wood, coal combustion
Yunker et al., 2002
(0.62)
(0.54)
Phe/Phe+Ant
Flu/Flu+Pyr
BaA/BaA+Chr
IP/IP+BghiP

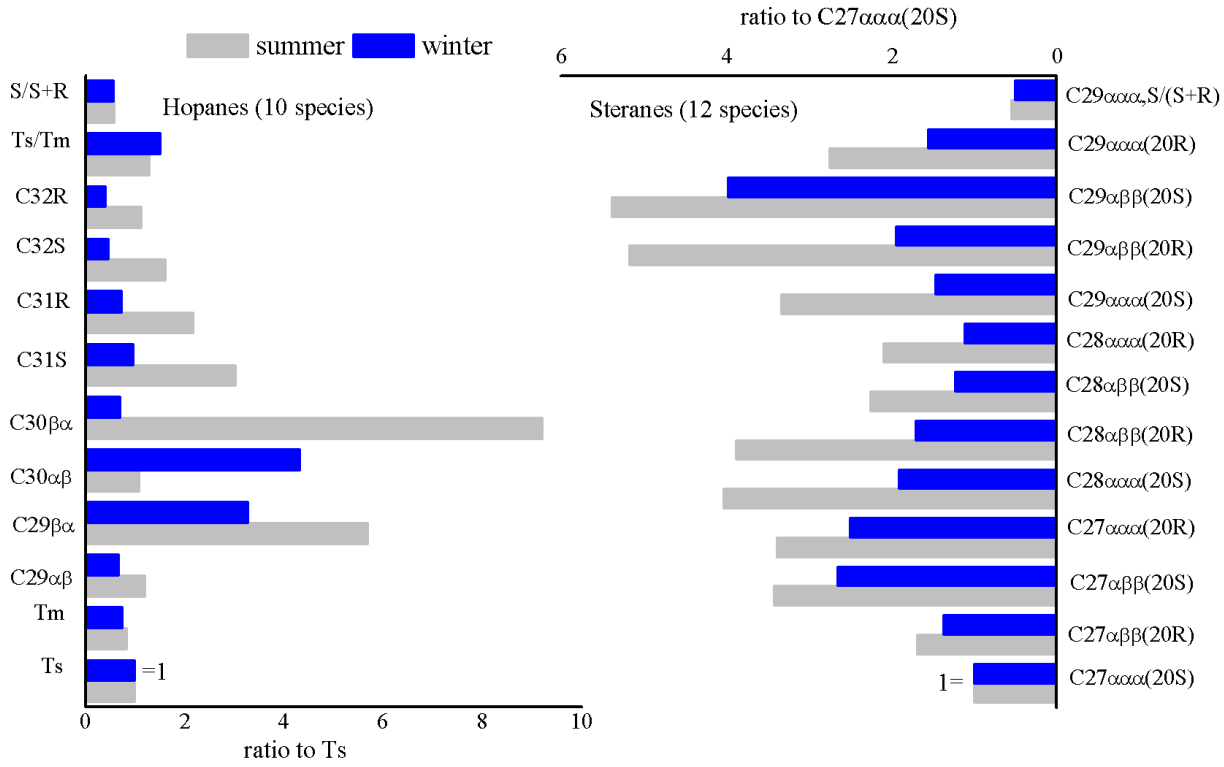
summer
winter
Hopanes (10 species)
S/S+R
Ts/Tm
C32R
C32S
C31R
C31S
C30βα
C30αβ
C29βα
C29αβ
Tm
Ts
=1
0
2
4
6
8
10
ratio to Ts
ratio to C27ααα(20S)
6
4
2
0
Steranes (12 species)
C29αααS/(S+R)
C29ααα(20R)
C29αββ(20S)
C29αββ(20R)
C29ααα(20S)
C28ααα(20R)
C28αββ(20S)
C28αββ(20R)
C28ααα(20S)
C27ααα(20R)
C27αββ(20S)
C27αββ(20R)
1=
C27ααα(20S)

1. Char/soot revealed dominance of biomass burning in winter and a major influence from fossil-fuel combustion in summer.
2. Air-soil/plant exchange contributed 2~3-ring PAHs in summer and biomass burning contributed 4-5-ring in winter.
3. Vehicle exhaust was the most common source of hopanes and steranes both in summer and winter.

Xi Wang, Ting Feng, Siyuan Zhang and Peili Lu performed the research; Fumo Yang, Jiaxin Liu and Zhigang Guo analyzed data; Fengwen Wang, Li Liu and Neil L. Rose wrote the paper. All the co-authors substantially contributed to commenting and revising it. All authors read and approved the final manuscript. The authors have declared no conflict of interest.